CrossMark

Carbon flows in eutrophic Lake Rotsee: a ^{13}C-labelling experiment

J. M. Lammers [ID] · **C. J. Schubert · J. J. Middelburg · G. J. Reichart**

Abstract The microbial segment of food webs plays a crucial role in lacustrine food-web functioning and carbon transfer, thereby influencing carbon storage and CO_2 emission and uptake in freshwater environments. Variability in microbial carbon processing (autotrophic and heterotrophic production and respiration based on glucose) with depth was investigated in eutrophic, methane-rich Lake Rotsee, Switzerland. In June 2011, ^{13}C-labelling experiments were carried out at six depth intervals in the water column under ambient light as well as dark conditions to evaluate the relative importance of (chemo)autotrophic, mixotrophic and heterotrophic production. Label incorporation rates of phospholipid-derived fatty acid (PLFA) biomarkers allowed us to differentiate between microbial producers and calculate group-specific production. We conclude that at 6 m, net primary production (NPP) rates were highest, dominated by algal photoautotrophic production. At 10 m —the base of the oxycline— a distinct low-light community was able to fix inorganic carbon, while in the hypolimnion, heterotrophic production prevailed. At 2 m depth, high label incorporation into POC could only be traced to nonspecific PLFA, which prevented definite identification, but suggests cyanobacteria as dominating organisms. There was also depth zonation in extracellular carbon release and heterotrophic bacterial growth on recently fixed carbon. Large differences were observed between concentrations and label incorporation of POC and biomarkers, with large pools of inactive biomass settling in the hypolimnion, suggesting late-/post-bloom conditions. Net primary production (115 mmol C m^{-2} d^{-1}) reached highest values in the epilimnion and was higher than glucose-based production (3.3 mmol C m^{-2} d^{-1}, highest rates in the hypolimnion) and respiration (5.9 mmol C m^{-2} d^{-1}, highest rates in the epilimnion). Hence, eutrophic Lake Rotsee was net autotrophic during our experiments, potentially storing large amounts of carbon.

J. M. Lammers (✉) · J. J. Middelburg · G. J. Reichart
Department of Earth Sciences, Utrecht University,
P.O. Box 80.021, 3508 TA Utrecht, The Netherlands
e-mail: j.m.lammers@uu.nl

C. J. Schubert
Department of Surface Waters Research and
Management, Eawag - Swiss Federal Institute of Aquatic
Science and Technology, Seestrasse 79,
6047 Kastanienbaum, Switzerland

G. J. Reichart
Department of Ocean Systems, NIOZ Royal Netherlands
Institute for Sea Research, Texel, P.O. Box 59,
1790 AB Den Burg, The Netherlands

Introduction

Within the global carbon cycle the cycling of organic matter in fresh-water systems has only recently been recognized as a significant component, potentially with global impacts (Battin et al. 2008, 2009; Cole et al. 2007; Raymond et al. 2013; Richey et al. 2002). Carbon loading to freshwater systems ranges between 1.9 and 2.9 Pg C y^{-1} (Battin et al. 2009; Cole et al. 2007; Tranvik et al. 2009), most of which is processed and/or stored within the system itself. Due to higher biological production and faster sedimentation rates compared to the oceans, lakes have a large storage capacity and bury as much as 30–60% organic carbon per year compared to oceanic carbon storage, despite their limited surface area relative to the ocean (Cole et al. 2007). Still, lakes are generally net sources of CO_2 to the atmosphere, with CO_2 evasion rates estimated to range between 0.75 and 2.1 Pg C y^{-1} (Battin et al. 2009; Cole et al. 2007; Tranvik et al. 2009).

Within lakes, carbon cycling is determined by in situ primary and secondary production, depending on nutrient availability and light, and also by inputs of terrestrial organic carbon and methane (either locally produced or derived via groundwater from surrounding soil). The availability of these different carbon sources has a major impact on food-web functioning and structure by affecting the relative amounts of primary and secondary production (Cole et al. 2006; Pace et al. 2004). The microbial segment of food-webs (phytoplankton and bacteria) therefore plays a crucial role in food-web functioning and transfer of organic matter through ecosystems to higher trophic levels (e.g. zooplankton, fish).

The microbial food web in particular is affected by present-day environmental changes in nutrient supply, oxygenation, temperature, light and atmospheric CO_2 levels (De Kluijver et al. 2013; Middelburg 2014; Travers et al. 2007) and must therefore be included in ecosystem studies. Most of these parameters vary with depth in freshwater ecosystems, allowing different microbial communities to occur simultaneously at different depths of the water column (Bossard et al. 2000; Galand et al. 2002; Humayoun et al. 2003; Koizumi et al. 2004; Øvreås et al. 1997). Hence, especially in stratified lakes, undersampling can easily lead to under- or overestimations of production and remineralization within different parts of the food web.

Different approaches have been used in the past, to investigate carbon processing in lakes, sometimes applying stable isotope ratios at natural abundances or after deliberate tracer additions (Brett et al. 2009; Cole et al. 2011; Pace et al. 2007). Under natural conditions, isotopic differences between substrates and consumers are typically small, and hence the isotopic signatures of producers often partially overlap. Adding 13C-label to enrich certain substrates enables quantification of carbon assimilation and the transfer of recently fixed carbon through the food web. Over the last years, the emergence of compound-specific stable isotope analyses (CSIA) has enabled including part of the microbial food web in ecological studies (Boschker et al. 1998; Middelburg et al. 2000; Van den Meersche et al. 2004). Specifically, biomarker molecules (mostly lipids) linked to specific (groups of) organisms are well suited for CSIA and have expanded our knowledge on microbial food-web functioning over a wide range of settings. Phospholipid-derived fatty acids (PLFAs) were used to differentiate between and zoom in on different primary producers (autotroph, mixotroph and chemoautotroph), secondary producers (heterotrophic bacteria) and detritus (dead organic matter) and to quantify group-specific production. PLFAs are produced by a wide variety of organisms, representing a wide range in trophic behavior. Although specific PLFAs do not uniquely represent one source organism, they can be very informative in labeling studies since DIC-derived enrichment directly or indirectly derives from autotrophic production, while DOC-derived enrichment of PLFAs results from heterotrophic production (Boschker et al. 1998; De Kluijver et al. 2013; Dijkman et al. 2009; Van den Meersche et al. 2004).

Here we contribute to further unravelling fluxes between lacustrine carbon pools and microbial groups using in situ 13C-labelling under both dark and light conditions at six different depth intervals in a shallow methane-rich, eutrophic lake (Rotsee, Switzerland). The incubations under ambient light conditions were labelled with 13C-bicarbonate to quantify total as well as group-specific primary production and to trace the

transfer of newly fixed carbon to bacteria. Dark incubations were labelled with ^{13}C-glucose, which is used as a substrate by the majority of heterotrophic producers and is therefore well suited to quantify heterotrophic bacterial turnover in terms of assimilation and respiration. Combining light and dark incubations thus allows for a more complete reconstruction of microbial carbon transfer. PLFA concentrations were compared to production rates and the relative importance of phytoplankton production and bacterial production and respiration was evaluated at different water depths, each with their own set of environmental conditions such as light penetration, nutrient availability and microbial community. This allowed for elucidating the most relevant processes at the different water depths, quantifying carbons flows through the microbial food web of a methane-rich, eutrophic lake.

Materials and methods

Study site

The experiment was carried out in Lake Rotsee, a prealpine Swiss lake. Rotsee (Fig. 1) is small (2.4 km long and 0.4 km wide), eutrophic and has a mean depth of 9 m and a maximum depth of 16 m. It has a drainage area of 4.6 km^2 and is fed by the Reuss-Rotsee canal, which draws from Reuss River. The lake is shielded from wind, allowing for the formation of a stable stratification from approximately May to November. Rotsee is monomictic and when stratified the oxycline is located between about 8 and 11 m, with an anoxic hypolimnion (Schubert et al. 2010). The lake is quite dark, with only 0.28% of light radiation reaching the oxycline, and 0.01% reaching 11 m depth (Oswald et al. 2015).

Rotsee has an intense methane cycle (Schubert et al. 2010); in the top few cm of sediment the methanogen acetoclastic *Methanosaeta* spp. is the main provider (>90%) of methane to the water column (Zepp Falz et al. 1999). It was found that during summer stratification, methane oxidation rates were highest within the oxycline with aerobic gammaproteobacterial methanotrophs (type I) being the main methane oxidizers, although alpha-methane oxidizing bacteria were also detected one year (Oswald et al. 2015). The aerobic oxidation of methane was found to be fuelled by light-dependent oxygenic photosynthesis (Oswald et al. 2015). Regardless, the epilimnion is still oversaturated in methane and thus serves as a source of methane to the atmosphere (Schubert et al. 2010).

Incubation experiments and sample collection

In situ ^{13}C-labelling experiments were carried out from June 10 to June 14, 2011. During the experiment, twelve pre-cleaned 25 L-bottles (transparent bottles:
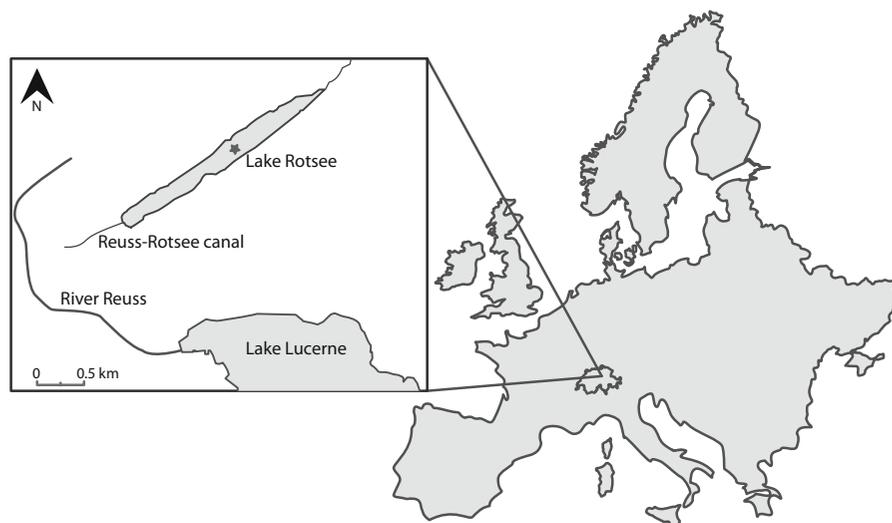
Fig. 1 Map showing the location of Lake Rotsee in Switzerland and its in- and outflowing rivers. Rotsee is connected to the river Reuss via the Reuss-Rotsee canal. The location of the experiment is indicated by a *star*

polycarbonate; dark bottles: low density polyethylene) were filled with water, which was retrieved from six different depths using Niskin bottles. At the site of the experiment, prior to collecting water, a CTD probe (Seabird SBE19) was deployed to measure in situ oxygen, temperature, conductivity and pH. The water was transferred from Niskin to incubation bottle on the ship using a tube, as quickly as possible, but some exchange with the atmosphere cannot be ruled out. Additionally, due to the shape of the caps, a small headspace remained in the incubation bottles. Clear bottles intended for light incubations were labelled with ^{13}C-Na-bicarbonate (8.4 mg > 98 at.% ^{13}C) and bottles for dark incubations were covered in water-proof aluminium-tape and labelled with ^{13}C-glucose (2.3 mg > 99 at.% ^{13}C), increasing DIC and DOC concentrations by about 0.16 and 1.0% respectively. Bottles were redeployed attached to a cable running from an anchor at the lake floor to a buoy, in such a way that each bottle was positioned at the original depth the incubated water was recovered from. The entire setup remained in situ for the four-day experiment. Before (T0) and after the experiment (T4), samples were collected from each bottle for oxygen, dissolved inorganic carbon (DIC), dissolved organic carbon (DOC), and particulate organic matter (POM) analyses.

Samples for dissolved oxygen analyses were fixed on site and measured by Winkler titration in the laboratory to ascertain the calibration of the CTD probe. Samples for DIC concentration and ^{13}C content were collected air-free in 20 mL headspace vials and sealed using airtight caps followed by mercury chloride poisoning. Samples were stored dark and upside down. Samples for DOC concentration and ^{13}C content were filtered through 0.45 μm GM/F filters and stored frozen (−20 °C) until further analysis. All remaining water was filtered through pre-weighed and pre-combusted GF/F filters (0.7 μm) for POM and the filter stored frozen (−20 °C) until extraction and further analysis.

Laboratory analyses

DIC concentrations were measured using a total organic carbon (TOC) analyzer (Shimadzu TOC-5050A), using an in-house seawater standard. A seawater standard is stable and can therefore also be used to check measurements of lacustrine DIC

samples. For δ^{13}C analyses of natural abundance and labelled DIC, a helium headspace was created and samples were acidified with a H_3PO_4 solution. Stable isotopes of the DIC were analyzed using a gas bench coupled on line to an IRMS (Thermo Delta V advantage) and were calibrated to the Vienna PeeDee Belemnite (V-PDB) scale using international (Li_2-CO_3) and in-house (Na_2CO_3) standards. For analyses of DOC concentration and δ^{13}C of the DOC, samples were treated and measured following Boschker et al. (2008) using high-performance liquid chromatography-isotope ratio mass spectrometry (HPLC-IRMS, Thermo Surveyor system). From the filters, the particulate organic carbon (POC) concentrations were measured using an elemental analyzer (EA) (Fisons Instruments NA1500) and the isotopic composition was analyzed on an EA-IRMS (Thermo Deltaplus). Carbon stable isotope ratios are expressed in the delta notation (δ^{13}C) with respect to the V-PDB standard. Precision is <0.35‰ based on international (Graphite quartzite standard NAXOS) and in-house (Nicotinamide) standards. No systematic changes were observed in the concentrations of DIC, DOC and DIC between T0 and T4. Therefore, concentrations are reported as averages of T0 and T4, of both transparent and dark incubations.

POM samples were freeze dried and lipids were extracted using a modified Bligh and Dyer method (Dickson et al. 2009). Total lipid extracts (TLE) were fractionated into simple lipids (SL), glycolipids (GL) and phospholipids (PL) on activated silicic acid columns using chloroform/acetic acid (100:1 v/v), acetone and methanol respectively as eluents (Dickson et al. 2009). Phospholipid fractions, containing phospholipid-derived fatty acids (PLFAs), were converted to fatty acid methyl esters (PL-FAME) by mild alkaline transmethylation (White et al. 1979). C12:0 and C19:0 FAME were added as internal standards. Concentrations and compound specific δ^{13}C of PL-FAME were determined using gas chromatography-combustion-isotope ratio mass spectrometry (GC-C-IRMS) using a column and oven program as described in Middelburg et al. (2000). Similar as for total carbon pools, no systematic changes were observed in PLFA concentrations between T0 and T4, hence concentrations are reported as averages of T0 and T4, of both light and dark incubations. Identification was based on comparing retention times using equivalent chain lengths. Carbon isotopic values were corrected for the

one added carbon during methylation using the carbon isotopic value of the derivatizing agent, which was determined offline.

Data analysis

Production rates (in mol L^{-1} d^{-1}) for carbon pools and PLFAs were calculated following de Kluijver et al. (2013) and Middelburg (2014) as

$$Production\ rate = \frac{\Delta^{13}F_{produced}}{\Delta^{13}F_{DIC}} \times \frac{C_{produced}}{t} \qquad (1)$$

where $C_{produced}$ is the concentration of the C species or PLFA that is produced in mol L^{-1}; t is the duration of the experiment and

$$\Delta^{13}F = {}^{13}F_{sample} - {}^{13}F_{background} \qquad (2)$$

With $^{13}F_{background}$ representing natural abundance ratios as measured at T0, before the label was added and where ^{13}F is the fraction ^{13}C, which is calculated as

$$\frac{^{13}C}{^{12}C + {}^{13}C} = \frac{R}{R+1} \qquad (3)$$

Isotope ratios R were derived from $\delta^{13}C$ values using

$$R = \left[\left(\delta^{13}C/1000\right) + 1\right] \times R_{VPDB} \qquad (4)$$

With $R_{VPDB} = 0.0111796$ (Coplen 2011). Only $\Delta\delta^{13}C$ values > 1.5‰ were considered for calculations, with

$$\Delta\delta^{13}C = \delta^{13}C_{sample} - \delta^{13}C_{background} \qquad (5)$$

Only bicarbonate-labelled incubations were corrected for $\Delta^{13}F_{DIC}$. For glucose-labelled incubations, the assumption was made that DOC was 100% labelled (see discussion).

PLFAs are produced by a wide variety of microbes. Branched PLFAs iC14:0, iC15:0 and aC15:0 all mainly derive from gram-positive bacteria (Kaneda 1991), although also occurring in some gram-negative bacteria (Zelles 1999). Here they are interpreted to represent bacteria in general. In Lake Rotsee, common phytoplankton PLFAs are C18:3ω3 (α-linolenic acid, or ALA), C18:4ω3 (stearidonic acid, or SDA) and C20:5ω3 (eicosapentaenoic acid, or EPA). These PLFAs are common in different phytoplankton phyla, e.g. Chlorophyta, Chrysophyta, Cryptophyta, Heterokontophyta, Haptophyta (Dijkman and

Kromkamp 2006; Taipale et al. 2013). PLFA C16:1ω7c is a common lipid in many organisms, including heterotrophic bacteria (Kaneda 1991), sulfur-oxidizing bacteria (van Gaever et al. 2009; Zhang et al. 2005), nitrifying bacteria (de Bie et al. 2002, Guezennec and Fialamedioni 1996; Lipski et al. 2001) and a range of phytoplankton species (Dijkman and Kromkamp 2006). C16:1ω7c has also been found in methane-oxidizing bacteria (Bodelier et al. 2009; Guckert et al. 1991).

Net primary production (NPP) was calculated using production rates of POC and DOC under light conditions. The percentage of extracellular release (PER) was calculated as the production of DOC divided by the total production (POC + DOC) under light conditions. Total label incorporation into POC in dark incubations was used to calculate glucose-based, heterotrophic production. Glucose-based respiration was calculated using total label transfer to the DIC pool in dark incubations. Steady-state was assumed for the calculation of these rates. Glucose-based bacterial growth efficiency (BGE) was calculated by dividing the concentration of labelled POC by the concentrations of labelled POC + DIC in dark incubations labelled with ^{13}C-glucose. The isotopic composition of the respired carbon was determined as the y-intercept of a linear trend line in a Keeling plot of 1/[DIC] versus natural abundance (T0) $\delta^{13}C_{DIC}$ for each depth.

Results

Oxygen and (in)organic carbon pools

Dissolved oxygen concentrations in Lake Rotsee are shown in Fig. 2a and clearly show the location of the oxycline between 7 and 10 m water depth, which corresponds well to earlier observations (Schubert et al. 2010). Oxygen concentrations in the epilimnion were ~400 µmol L^{-1}, while oxygen concentrations in the hypolimnion were below 10 µmol L^{-1}, with values close to zero at 15 m depth, near the lake floor.

Average POC concentrations (Fig. 2b) were relatively stable throughout the epilimnion, with values ranging from 41 to 57 µmol L^{-1}. From 8.5 m down to the maximum depth of 15 m, POC concentrations rose to 215 µmol L^{-1}. Average DOC concentrations (Fig. 2c) decreased with depth in the epilimnion from 370 to 300 µmol L^{-1}, then increased to
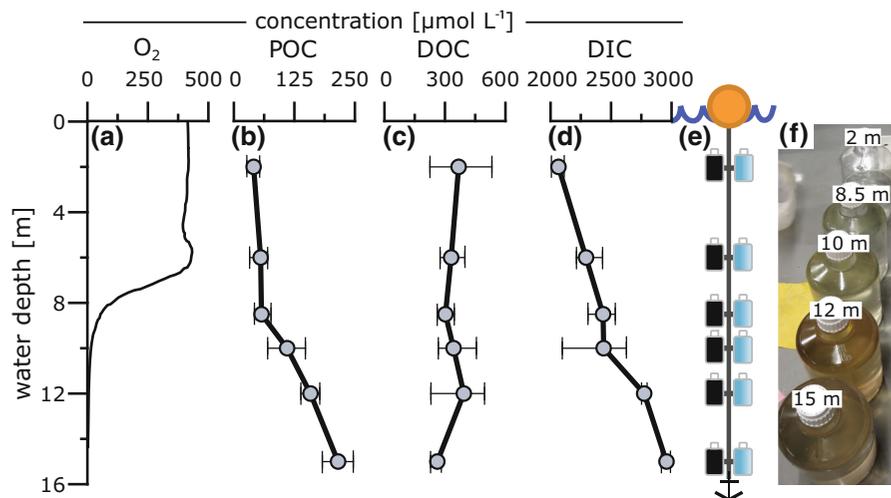
Fig. 2 Concentrations in μmol L^{-1} of **a** oxygen, **b** POC, **c** DOC and **d** DIC. Concentrations of POC, DOC and DIC are averages of T0 and both light and dark incubations; **e** the experimental set-up showing two bottles at each sampling depth: one dark bottle in which glucose was labelled and one transparent bottle in which bicarbonate was labelled (bottle size is not to scale); **f** Light incubation bottles derived from 2, 8.5, 10, 12 and 15 m water depth, showing an increase in suspended matter concentration with depth. The bottle from 6 m water depth was being processed at the time this picture was taken

390 μmol L^{-1} between 8.5 and 12 m and were lowest at 15 m (260 μmol L^{-1}). It should be noted that as a result of the 0.45 μm pore size of the filters used for DOC sampling ("Incubation experiments and sample collection" section), bicarbonate-based fixation by small, free-living microbes might also contribute to the DOC results. However, given the high DOC concentrations and production rates (see below), it seems unlikely that these small microbes had a large effect on calculated fluxes. Average DIC concentrations (Fig. 2d) increased with depth from 2.1 mmol L^{-1} at 2 m to 3.0 mmol L^{-1} at 15 m.

All PLFA concentrations showed the same overall trend, with low concentrations in the epilimnion, a strong increase in the chemocline and highest values reached in the hypolimnion at either 12 or 15 m water depth. This pattern closely mimics the changes observed in POC concentration. PLFAs iC14:0, iC15:0 and aC15:0 (Fig. 3a–c) all showed peak concentrations at 15 m, with iC14:0 reaching 0.015 μmol C L^{-1}, and both iC15:0 and aC15:0 reaching highest values of 0.07 μmol C L^{-1}. PLFA C16:ω7c (Fig. 3d) showed the same trend as the iso- and anteiso PLFAs: peaking at 15 m with a maximum concentration of 1.04 μmol C L^{-1}. PLFAs C18:3ω3, C18:4ω3 and C20:5ω3 (Fig. 3e–g) showed the same trend, peaking at 0.05, 0.02 and 0.02 μmol C L^{-1}

respectively at 12 m and reaching values of 0.04, 0.01 and 0.01 μmol C L^{-1} at 15 m.

Tracer assimilation under light conditions

Because the same amount of ^{13}C-bicarbonate label was added at each depth whereas the DIC concentration varied, δ^{13}C enrichment of the DIC varied from 115 to 160‰ at the different depths, depending on initial DIC concentration (Fig. 2d) (Table S1). At T4, the δ^{13}C of DOC appreciably increased between 6 and 10 m by 13 to 24‰ (data not shown). Similarly, the δ^{13}C of POC increased appreciably between 2 and 10 m by 6 and 84‰ (data not shown). Production rates per day for DOC and POC showed that label incorporation into POC was strongest at 2 m (6.9 μmol C L^{-1} d^{-1}) and decreased with depth to zero at 12 m (Fig. 4a). Label transfer to DOC was zero at 2 m, increasing to 12.6 μmol C L^{-1} d^{-1} at 6 m, remaining high at 8.5 and 10 m (7.2 and 11.0 μmol C L^{-1} d^{-1} respectively) and decreasing again to zero at 12 and 15 m depth. A ^{13}C mass balance for inorganic and organic carbon pools was achieved within 15%, which is acceptable for our purposes.

For PLFAs iC14:0, iC15:0 and aC15:0 (Fig. 5a–c, grey squares for light incubations), absolute label

Fig. 3 PLFA biomarker concentrations in μmol C L⁻¹ of **a** iC14:0, **b** iC15:0, **c** aC15:0, **d** C16:1ω7c, **e** C18:3ω3, **f** C18:4ω3, and **g** C20:5ω3. PLFAs in graphs **a–c** are produced by bacteria, PLFA C16:1ω7c is common in many microbial groups, and PLFAs in graphs **e–g** derive from phytoplankton. Concentrations are averages of T0, light and dark incubations
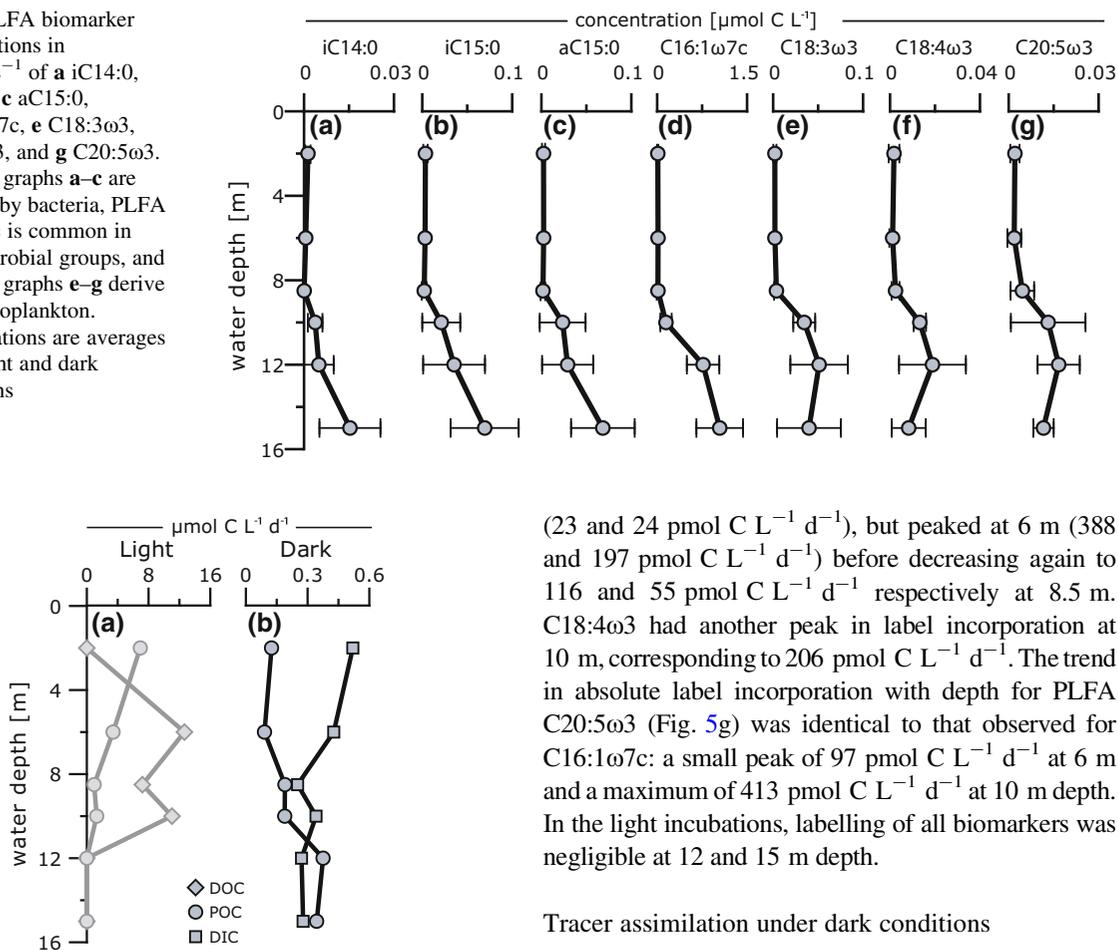

Fig. 4 Production rates with depth of POC, DOC and DIC in μmol C L⁻¹ d⁻¹ under **a** light and **b** dark conditions

incorporation was only observed in the upper 8.5 m. PLFA iC14:0 (Fig. 5a) had a maximum production rate, corresponding to 32 pmol C L⁻¹ d⁻¹ at 2 m, which decreased to zero at 8.5 m. Label incorporation into iC15:0 (Fig. 5b) corresponded to 35 pmol C L⁻¹ d⁻¹ at 2 m, increasing to 68 pmol C L⁻¹ d⁻¹ at 8.5 m. For PLFA aC15:0 (Fig. 5c) this was 32 pmol C L⁻¹ d⁻¹ at 2 m, decreasing to zero at 6 m and reaching a maximum value of 47 pmol C L⁻¹ d⁻¹ at 8.5 m. Production of PLFA C16:1ω7c (Fig. 5d) was highest of all PLFAs, with values of 208 pmol C L⁻¹ d⁻¹ at 2 m, increasing to 1326 pmol C L⁻¹ d⁻¹ at 6 m, then decreasing to 626 pmol C L⁻¹ d⁻¹ at 8.5 m with highest values observed at 10 m, which corresponds to 4229 pmol C L⁻¹ d⁻¹. PLFAs C18:3ω3 and C18:4ω3 (Fig. 5e, f) showed only minor label incorporation at 2 m

(23 and 24 pmol C L⁻¹ d⁻¹), but peaked at 6 m (388 and 197 pmol C L⁻¹ d⁻¹) before decreasing again to 116 and 55 pmol C L⁻¹ d⁻¹ respectively at 8.5 m. C18:4ω3 had another peak in label incorporation at 10 m, corresponding to 206 pmol C L⁻¹ d⁻¹. The trend in absolute label incorporation with depth for PLFA C20:5ω3 (Fig. 5g) was identical to that observed for C16:1ω7c: a small peak of 97 pmol C L⁻¹ d⁻¹ at 6 m and a maximum of 413 pmol C L⁻¹ d⁻¹ at 10 m depth. In the light incubations, labelling of all biomarkers was negligible at 12 and 15 m depth.

Tracer assimilation under dark conditions

Since the initial concentrations of DOC varied with depth and equal amounts of ¹³C-glucose were added to the dark incubation bottles, the δ¹³C increase of DOC varied from 512 to 1119‰ for the different bottles (Table S1). The absolute transfer of label from DOC to DIC (Fig. 4b), indicating respiration of added glucose, was highest at 2 and 6 m, with values corresponding to 0.52 and 0.43 μmol C L⁻¹ d⁻¹ respectively. In and below the chemocline, absolute label transfer to DIC was relatively constant at 0.25–0.28 μmol C L⁻¹ d⁻¹, with the exception of a small peak at 10 m corresponding to 0.34 μmol C L⁻¹ d⁻¹. Label transfer to POC reflects heterotrophic production in the epilimnion and was 0.12 and 0.09 μmol C L⁻¹ d⁻¹ at 2 and 6 m respectively, with values increasing to 0.19 μmol C L⁻¹ d⁻¹ in and just below the chemocline. Label incorporation values for POC were highest in the hypolimnion reaching 0.38 μmol C L⁻¹ d⁻¹ at 12 m and 0.34 μmol C L⁻¹ d⁻¹ at 15 m. Also in these
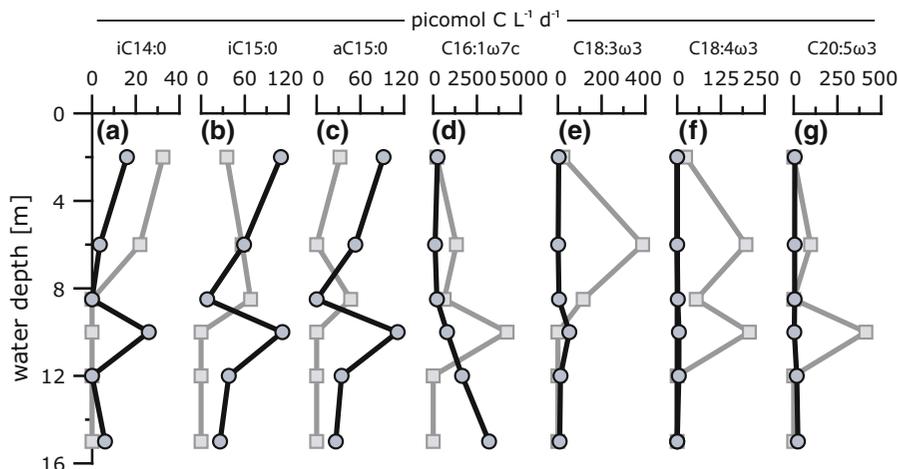
Fig. 5 Production rates of PLFA biomarkers in picomol C L^{-1} d^{-1} of **a** iC14:0, **b** iC15:0, **c** aC15:0, **d** C16:1ω7c, **e** C18:3ω3, **f** C18:4ω3 and **g** C20:5ω3. PLFAs in graphs **a–c** are produced by bacteria, PLFA C16:1ω7c is common in many microbial groups, and PLFAs in graphs **e–g** derive from phytoplankton. *Grey squares* represent incubations under light conditions. *Black circles* represent dark incubations

incubations, mass balance for inorganic and organic carbon pools was achieved within 15%, which is again acceptable for our purposes.

Similar patterns were observed for PLFAs iC14:0, iC15:0 and aC15:0 (Fig. 5a–c with black circles representing dark incubations). Incorporation decreased with depth in the epilimnion from 16, 110 and 92 pmol C L^{-1} d^{-1} respectively at 2 m depth to zero at 8.5 m. All three showed a peak in incorporation at 10 m (26 pmol C L^{-1} d^{-1} for iC14:0; 112 pmol C L^{-1} d^{-1} for iC15:0 and aC15:0), decreasing to lower values deeper in the hypolimnion. In the dark incubations label incorporation was highest for PLFA C16:1ω7c (Fig. 5d), showing relatively low values in the epilimnion and at 8.5 m, varying between 109 and 249 pmol C L^{-1} d^{-1}, then increasing with depth to a maximum value of 3200 pmol C L^{-1} d^{-1} at 15 m. For PLFAs C18:3ω3 and C18:4ω3 (Fig. 5e, f), production rates in the dark incubations were very low throughout the water column, with maximum values corresponding to 12 pmol C L^{-1} d^{-1}, with the exception of a peak in C18:3ω3 at 10 m depth of 52 pmol C L^{-1} d^{-1}. Label incorporation rates for PLFA C20:5ω3 (Fig. 5g) were low as well, between 5.1 and 6 pmol C L^{-1} d^{-1} between 2 and 8.5 m water depth, increasing to a maximum of 24 pmol C L^{-1} d^{-1} at 15 m, which is similar to the trend observed for PLFA C16:1ω7c.

Production and respiration

Net primary production (NPP, the sum of label transfer from DIC to POC and DOC, Table 1) was highest at 6 m with a rate of 16.0 μmol C L^{-1} d^{-1}, decreasing with depth to 8.1 μmol C L^{-1} d^{-1} at 8.5 m. At 10 m water depth, NPP was somewhat higher with a value of 12.3 μmol C L^{-1} d^{-1}, decreasing to zero at 12 and 15 m depth. From 6 to 10 m depth label transfer from DIC to DOC was substantial, resulting in high percentages of extracellular relase (Table 1) increasing from 78.8% at 6 m to 89.6% at 10 m water depth. In the epilimnion and chemocline, glucose-based, heterotrophic production (Table 1) was much lower than NPP, with rates between 0.12 and 0.19 μmol C L^{-1} d^{-1}. Heterotrophic production rates were somewhat higher in the hypolimnion (0.38 to 0.34 μmol C L^{-1} d^{-1} at 12 and 15 m respectively). Bacterial growth efficiency (Table 1), the production of bacterial biomass relative to the total amount of glucose-^{13}C substrate assimilated (Del Giorgio and Cole 1998), also increased with depth from 0.19 at 2 m to 0.55 at 15 m water depth.

Respiration rates (Table 1) were highest in the epilimnion, corresponding to values of 0.52 and 0.43 μmol C L^{-1} d^{-1} at 2 and 6 m respectively, decreasing to rates between 0.25 and

Table 1 Net primary production, glucose-based production and glucose-based respiration in µmol C L^{-1} d^{-1}, and percentages of extracellulare release and bacterial growth efficiency with depth

Water depth (m)	Net primary production (µmol C L^{-1} d^{-1})	Percentage extracellular release (PER)	Glucose-based production (µmol C L^{-1} d^{-1})	Bacterial growth efficiency	Glucose-based respiration (µmol C L^{-1} d^{-1})
2	6.93	0.00	0.12	0.19	0.52
6	16.05	78.8	0.09	0.17	0.43
8.5	8.15	88.4	0.19	0.43	0.25
10	12.32	89.6	0.19	0.36	0.34
12	0.00	–	0.38	0.58	0.27
15	0.00	–	0.34	0.55	0.28
Depth-integrated rates (µmol C L^{-1} d^{-1})	115	–	3.3	–	5.9

0.28 µmol C L^{-1} d^{-1}, with the exception of 10 m depth, where respiration was slightly higher with a rate of 0.34 µmol C L^{-1} d^{-1}. From unlabelled samples, using a Keeling plot (Fig. 6), it was derived that the respired DIC had an average δ^{13}C value of −21.8‰.

Discussion

Before discussing the results of the labelling experiments in detail, it is informative to first review the methodology used in this study. In our experiments glucose was added as a tracer to the dark incubations to quantify bacterial production rates and, given the complex and largely unknown composition of the natural DOC pool, it is not possible to extrapolate glucose-based rates to bulk DOC processing rates. Moreover, glucose is probably more readily usable as a substrate compared to the naturally available DOC,

Fig. 6 Keeling plot showing 1/(DIC concentration) vs. the natural abundance value (T0) of δ^{13}C$_{DIC}$. The y-intercept of the linear trendline indicates the δ^{13}C of respired carbon

likely resulting in an overestimation of assimilation and respiration rates. Conversely, some microbes do not use glucose as a substrate, and their production and respiration could not be traced. To quantify these effects would require dedicated experiments using a range of different substrates, which is beyond the scope of this research. Hence the rates of assimilation and respiration in the dark experiments discussed here are potential rates and represent glucose-based bacterial production and respiration.

Using PLFAs in isotope-labelling experiments allowed us to distinguish between metabolic pathways in the microbial communities. Still, there are limitations to what PLFAs can tell us about certain microbial groups. In this study, we were unable to identify cyanobacteria, which mostly produce non-unique PLFAs (Gugger et al. 2002). Although not produced by all cyanobacteria species (Gugger et al. 2002), the more specific PLFA C18:3ω6, which has previously been used as a marker for cyanobacteria, was either not present or detected in very low abundances in our samples. Heterocyst glycolipids (HGs) have also been studied as cyanobacterial markers (Bauersachs et al. 2009), but due to the work-up process prior to PLFA analyses it was unfortunately no longer possible to analyse HGs on our samples. Also, we were unable to trace methanotrophic bacteria using PLFAs. Specific PLFAs in methanotrophic bacteria are C16:1ω8c and C16:1ω5t for type I, while for type II C18:1ω8c (Bowman et al. 1991, 1993; Nichols et al. 1985) and also C18:2ω7c,12c and C18:2ω6c,12c (Bodelier et al. 2009) are considered biomarker PLFAs. In the samples from Lake Rotsee, none of the methanotrophic PLFAs
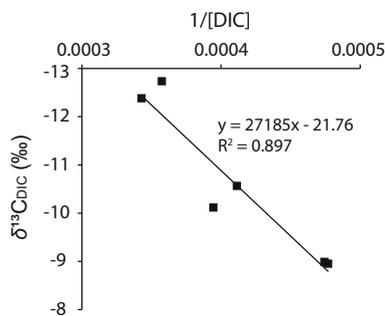
were detected in quantities that allow for reliable isotope analysis. Only C18:2ω6c was detected, but both concentrations and enrichment values were low.

The incubation experiments were performed at multiple depths, but at a single location. Consequently, these incubations did not capture any potential horizontal spatial heterogeneity. Still, horizontal spatial differences are expected to be relatively small given the narrow shape of the lake. The incubation experiments lasted four days and the light treatment hence included natural day-night cycles. The four-day duration of the experiments was a compromise between detecting activity of slow-growing organisms on the one hand and preventing changes in environmental conditions, substrate depletion and isotope scrambling on the other hand (Middelburg 2014). Concentrations of carbon pools and PLFAs did not significantly change over four days, suggesting steady-state conditions. However, only 2 to 32% of the added ^{13}C-glucose remained at T4, implying that glucose-based production and respiration rates may have been underestimated, in particular at depths 12 and 15 m where more than 97% was processed. Although we did not measure oxygen concentrations at T4, we have no indication of oxygen limitation in the oxygenated epilimnion. Only at the interface between oxygenated and anoxic water (8.5 m water depth), the small headspace that was present over the incubated sample, might have caused a switch in the microbial community. Since our experiment was carried out once, it is possible that on a longer timescale, the calculated rates and their relative importance in Lake Rotsee differ.

Carbon flows

Concentrations of POC were relatively low in the surface layers compared to deeper in the water column (Fig. 2b) possibly related to post and/or late-bloom conditions as debris of the bloom still remained at depth. This is not surprising since the experiment was performed in June when stratification is stable, the chemocline is well established and production rates are still high. Visual inspection of the incubated water and the filtered material showed a strong increase in the amount of suspended material with depth (Fig. 2f). Additionally, the observed increase in POC and PLFA concentrations in the hypolimnion is in line with settling of large amounts of organic matter during post and/or late-bloom conditions.

Label incorporation into POC and subsequent transfer to DOC under light conditions (Fig. 4a) together constitute net primary production (Table 1). Labelling of POC is in line with expected decreasing production with depth, as light conditions become less favorable for photosynthesis. After the four-day experiment, label incorporation into POC showed a somewhat smaller uptake than labelling of DOC (Fig. 4a). In short-term ^{13}C-bicarbonate tracer experiments label transfer to DOC reflects exudation of organic carbon (EOC), which is the release of excess organic molecules by phytoplankton when carbon fixation is higher than incorporation into new cell material (Fogg 1983) and is generally highest under nutrient-poor conditions, when growth of phytoplankton is limited, but photosynthetic carbon fixation is not (Fogg 1983; Van den Meersche et al. 2004). For Lake Rotsee, EOC as a percentage of NPP (PER) is very high (Table 1), but it has been shown that the epilimnic nitrate content decreases to very low concentrations after spring and nitrite concentrations are low throughout the year (Schubert et al. 2010). Despite the overall eutrophic state of the lake, nutrient poor post-/late-bloom conditions at the time of the incubation experiments may have favored exudation of organic carbon by algae, causing the DOC pool to become labelled at several depths.

Production of labelled POC in the dark incubations (Fig. 4b) represents heterotrophic production (Table 1, see above) and was relatively stable in the epilimnion, but increased in the hypolimnion as a result of more favorable conditions: less competition from other producers and increased nutrient availability. Compared to NPP, the potential heterotrophic production rates in the epilimnion and chemocline were substantially lower (Table 1). When integrated over the water column, the daily rate of net primary production was 115 mmol C m^{-2} d^{-1}, while the potential rate of heterotrophic production was only 3.3 mmol C m^{-2} d^{-1}.

Crucially important when studying net ecosystem metabolism is the relative rate of production compared to respiration as a function of water depth (Pace and Prairie 2005). Within heterotrophic lakes allochthonous carbon may stimulate part of the food web (Battin et al. 2008; Brett et al. 2009; Cole et al. 2006; Pace et al. 2004), resulting in higher rates for respiration than for primary production. This will lead to (1) oxygen diffusing into the lake since dissolved oxygen

levels become lower than atmospheric levels and (2) the partial pressure of CO_2 increases to higher levels than in the atmosphere, causing it to diffuse out of the lake (Prairie et al. 2002). It has been found that many aquatic systems are net heterotrophic (Cole et al. 2000; Del Giorgio and Peters 1994; Del Giorgio et al. 1997), which may also be expected for Lake Rotsee, given its strong methane cycle (Schubert et al. 2010). The glucose-based respiration rate integrated over the water column was 5.9 mmol C m^{-2} d^{-1} in Lake Rotsee. The resulting difference between NPP and respiration is quite large ($\sim$109 mmol C m^{-2} d^{-1}) indicating that, despite the uncertainties in glucose-based respiration, Lake Rotsee was net autotrophic during our experiment. However, our assessment of the carbon flows is incomplete because high methane fluxes from the sediment and intense methane cycling in the water column should also be considered in the overall carbon balance. Moreover, as a consequence of the high rate of NPP, there was a large flux of organic matter to the sediment. Within the sediment, this organic matter will be processed, releasing methane to the overlying water column. Although unexpected, given that many lakes are net heterotrophic as mentioned above, the observed large difference between NPP and potential respiration in Lake Rotsee still falls within the range of net ecosystem productivity found among lakes and years by Cole et al. (2000), who observed daily rates up to +175 mmol C m^{-2} d^{-1}.

Respiration added DIC with a δ^{13}C of -21.8‰, while the DOC pool from which it was derived had a δ^{13}C of about -25‰ (Supplementary material online), suggesting preferential degradation of heavy compounds such as sugars and also certain amino acids (Scott et al. 2006). Moreover, the relatively heavy signature of the substrate excludes a substantial contribution of soil derived organic matter, which consists mainly of trees, ferns, shrubs, reed and grassland (Naeher et al. 2014), which is generally isotopically depleted. This is in line with the observed low glucose-based respiration rates in Lake Rotsee.

Phytoplankton production

Photoautotrophy Enrichment of phytoplankton PLFAs (C18:3ω3, C18:4ω3 and C20:5ω3) in the bicarbonate-labelled (light) incubations (Fig. 5e–g) derives from autotrophic production. The highest

concentrations of autotrophic biomass were observed below the chemocline (Fig. 3e–g), similar to the other PLFA biomarkers (Fig. 3a–d) and in line with post-/late-bloom conditions as suggested above. Light conditions below the chemocline are not favorable for typical photoautotrophic production, implying that this biomass can fix little amounts of carbon. This is corroborated by the labelling experiment, showing that production rates of phytoplankton PLFAs (Fig. 5e–g) were in line with the epilimnion being the main site for photoautotrophic production, with maximum production values reached at a water depth of 6 m. Maximum production values at 6 m are in agreement with maximum Chlorophyll α concentrations found in Lake Rotsee around this depth in June by (Brand et al. 2016). At 6 m depth, photoautotrophs therefore seem to have been the dominant producers. The high production levels at 6 and 10 m mainly resulted in labelling of DOC (Fig. 4a). The low epilimnic algal biomarker concentrations imply that the biomass present was very active and, moreover, that recycling of biomass must have been important in the epilimnion. An intense internal nutrient cycle in Rotsee has been suggested by (Bloesch et al. 1977), who calculated that 35–75% of the nitrogen and 55–85% of the phosphorous required for primary production can be regenerated.

Based on the production rates of C18:3ω3, C18:4ω3 and C20:5ω3, photoautotrophy seems minor at 2 m water depth (Fig. 5). In contrast, Fig. 4a shows highest POC label incorporation at 2 m. Evidently, another primary producer, not represented by the PLFA biomarkers studied here (see above), dominated production at this depth. Cyanobacteria are the most likely candidates, as they are ubiquitous photosynthesizers and have been found to account for 99% of total cell counts in 2013 (Brand et al. 2016). High cyanobacterial growth rates are in accordance with the observed lack of label transfer to the DOC pool at 2 m depth (Fig. 4a). Hence it is possible that cyanobacterial production is responsible for the observed high levels of label incorporation into POC and insignificant transfer to DOC at 2 m depth.

Light penetration in Lake Rotsee decreases to $\pm$ 0.28% of surface light intensity at the oxycline and 0.01% at 11 m depth (Oswald et al. 2015). At water depths less than 10 m production of PLFAs C18:3ω3, C18:4ω3 and C20:5ω3 was detected (Fig. 5e,f,g). At 10 m water depth, only C18:4ω3

and C20:5ω3 were produced and no C18:3ω3. These results confirm an earlier report that oxygenic primary production (assumed to derive from oxygenic photoautotrophs) has been detected at and below the oxycline (Oswald et al. 2015). Moreover, our data suggest that the primary producer community differed in this low light zone. Rhodophyta are a possible candidate as these algae are known to exhibit low-light adapted photosynthesis (Necchi and Zucchi 2001) and produce C18:4ω3 and C20:5ω3 but not C18:3ω3 (Dijkman and Kromkamp 2006).

Chemoautotrophy Anaerobic and potentially aerobic chemoautotrophy occur in the water column of Lake Rotsee, since sulphate, sulfide and ammonium have been detected (Schubert et al. 2010). In the past, rates of chemoautotrophic bacterial production (CBP) in other lakes were calculated using data from DIC labelled incubations in bottles covered with aluminium foil (Hama et al. 1983; Morana et al. 2016). Since in our setup DIC-labelled incubations were carried out under light conditions only naturally dark depths (see above) are potentially suitable to calculate chemoautotrophic DIC uptake. As mentioned before, photoautotrophic production at 8.5 and 10 m has been detected at and below the oxycline in Lake Rotsee.

An estimate of chemoautotrophic production may still be made based on label incorporation into PLFAs. The redox gradients in the chemocline (8.5–10 m water depth) are the most likely location for chemoautotrophy. It can be observed in Fig. 5 that in addition to phytoplankton-derived PLFAs, also bacterial PLFAs iC14:0, iC15:0 and aC15:0 were labelled at 8.5 m depth and PLFA C16:1ω7c was labelled at 8.5 and 10 m depth. The observed incorporation of labelled carbon in the bacterial PLFAs at 8.5 m water depth (Fig. 5a–c) could result from heterotrophic assimilation of organic carbon exuded by phytoplankton or from chemoautotrophic production and we cannot be certain about the relative contributions of each. At 10 m water depth, no production of branched PLFAs was observed and hence at this depth labelling of C16:1ω7c is indicative of chemoautotrophy. Moreover, a comparison between the production rates of C16:1ω7c and other phytoplankton PLFAs, allows us to differentiate between low-light photosynthetic versus chemoautotrophic production of C16:1ω7c. In phytoplankton, C16:1ω7c contributes to a smaller or similar extent to total PLFAs as other PLFAs such as C18:4ω3 and C20:5ω3 (Dijkman and Kromkamp

2006), which also showed label incorporation at 10 m. Highest fractions of C16:1ω7c are found in Heterokontophyta, which produce similar amounts of C16:1ω7c and C20:5ω3. However, both production rates and concentrations of C16:1ω7c were (at least) 10 times higher compared to C20:5ω3: concentrations were 0.15 versus 0.013 μmol C L^{-1} (Fig. 3d, g) and production rates were 4230 versus 413 pmol C L^{-1}·d^{-1} (Fig. 5d, g). This indicates that at 10 m water depth, at most 10% of the peak in labelling of C16:1ω7c can be explained by low-light adapted photosynthesis. The remainder most likely derived from chemoautotrophic production by sulfur-oxidizers and/or nitrifiers, which is in line with the observed lack in labelling at 12 and 15 m depth (Fig. 5), as these are both obligate aerobes.

Methanotrophy Given that Lake Rotsee has a strong methane cycle and that methane-oxidizing bacteria have previously been detected in the water column (Oswald et al. 2015; Schubert et al. 2010), it should be kept in mind that C16:1ω7c has also been found in some methane-oxidizing bacteria (Bodelier et al. 2009; Guckert et al. 1991). In fact, highest methane oxidation rates, attributed to type I MOB, were found at and below the oxycline (Oswald et al. 2015), at the same depth of highest (chemo)autotrophic production rates of C16:1ω7c (Fig. 5d). The natural abundance δ^{13}C value of C16:1ω7c (and other nonspecific PLFAs) showed a shift towards more depleted values at 8.5 and 10 m (data not shown), which is the zone identified as having highest methane-oxidation rates by Oswald et al. (2015). Hence, a partially methanotrophic origin for these PLFAs cannot be ruled out, in which case the calculated production rates represent minimum values as the isotopic signal may have been mixed with ^{13}C-depleted methane-derived carbon.

Mixotrophy The ability of phytoplankton to switch facultatively between DIC and DOC as substrates for the production of biomass is called mixotrophy (or phagotrophy). Many organisms are capable of mixotrophy, albeit to differing degrees. In our experiment, mixotrophy is observed when transfer of label to phytoplankton PLFAs occurs not only in bicarbonate-labelled light incubations but also in glucose-labelled dark incubations. From Fig. 5e, f it is clear that only PLFA C18:3ω3 with a glucose-based production rate of 52 pmol L^{-1} d^{-1} at 10 m could have a mixotrophic source at this water depth. Since its producers Cryptophyta and Dinophyta, are known to

be mixotrophic (Jones et al. 1994; Roberts and Laybourn-Parry 1999; Sanders and Porter 1988) these are potential source organisms for this PLFA at 10 m water depth, as are diatoms. Diatoms are primarily photoautotrophic, although some also exhibit heterotrophic behavior dependent on conditions (e.g. limited light availability, high DOC concentrations) (Lewin 1953). Additionally, heterotrophic production of PLFA C20:5ω3 by diatoms provided with glucose as a source of carbon and energy has been demonstrated (Shishlyannikov et al. 2014; Tan and Johns 1996). It is noteworthy that in our experiment PLFA C20:5ω3, which derives from diatoms, Cryptophytes and Dinophyta, did not show glucose-based production (Fig. 5g). This implies that C20:5ω3 is only produced autotrophically in Lake Rotsee, confirming our earlier suggestion that C20:5ω3 has a different source organism than C18:3ω3.

Heterotrophic bacterial production

Heterotrophic production, or production of PLFAs in glucose-labelled incubations, was eminent in bacteria-derived PLFAs iC14:0, iC15:0, aC15:0 (Fig. 5a–c) and also in C16:1ω7c (Fig. 5d). Below the chemocline, production of C16:1ω7c only occurred in dark, glucose-labelled incubations, attesting to heterotrophic production.

Glucose-based production rates of PLFAs iC14:0, iC15:0 and aC15:0 (Fig. 5a–c) matched the DOC concentration profile (Fig. 2c), with high rates at 2 m, which decreased with depth until 8.5 m. Similarly, following high DOC concentrations and high (glucose-based) bacterial growth efficiencies (Table 1) in the hypolimnion, high bacterial production rates were also expected for 12 and 15 m water depth. This was however not the case, suggesting that in the hypolimnion the bacteria that produce PLFAs iC14:0, iC15:0 and aC15:0 were outcompeted by the heterotrophic source organism of C16:1ω7c.

Labelling of bacterial PLFAs in light incubations indirectly derives from autotrophic production, via consumption of exuded organic carbon (assuming bacteria do not feed directly on labelled phytoplankton). So far, no indication has been found that the exuded substances are used as a substrate by phytoplankton itself or that it significantly contributes to their growth (Fogg 1983), leaving the exudates altogether available for utilization by heterotrophic producers. Organic carbon exudates mainly consist of glycolic acid (Fogg 1983), which can be respired and taken up by many bacterial species. Growth yield, however, seems to be low (Fogg 1983; Smith et al. 1977; Wright and Shah 1975) and it has been suggested that glycolic acid functions as a co-metabolite, providing energy for the assimilation of other substances (Wright and Shah 1975). In Lake Rotsee, however, label transfer to heterotrophic bacteria in the DIC-labelled incubations resulted in relatively high production rates (compared to glucose-based production rates). This shows that at 2 m, even though phytoplankton production based on PLFA-labelling seems low, there was substantial uptake of labelled carbon by bacteria. Since no label was recovered in the DOC pool at this depth, it appears that heterotrophic bacteria were feeding on organic carbon produced by the inferred cyanobacteria, suggesting that their growth is tightly coupled at 2 m depth. Alternatively, the much larger pool of refractory DOC may obscure rapid turnover of labile DOC used by bacteria as a substrate. Below 10 m water depth, heterotrophic producers did not show an appreciable uptake of bicarbonate label, as expected for 12 and 15 m, since no label was incorporated into phytoplankton biomass or DOC. At 10 m however, the DOC pool became substantially labelled (Fig. 4a), but the heterotrophic bacteria did not (Fig. 5a–c). Although it may have been used as a co-metabolite, other substances were used for growth, since incorporation of labelled glucose in the dark incubations showed (maximum) DOC uptake at 10 m water depth.

Conclusions and implications

By combining the tracer experiments with compound-specific stable isotope analyses of PLFAs we were able to identify and quantify the metabolic processes that affect the concentration and composition of DOC, DIC and POC pools at each depth. Figure 7 shows the main production types with depth, with photoautotrophic production dominating at 2 and 6 m, chemoautotrophic production dominating at 10 m depth and glucose-based heterotrophic production being most important at 12 and 15 m. At 8.5 m water depth, production rates of PLFAs showed that multiple processes occurred simultaneously. Furthermore we showed that the depth-dependence of primary production is also reflected in the microbial communities,
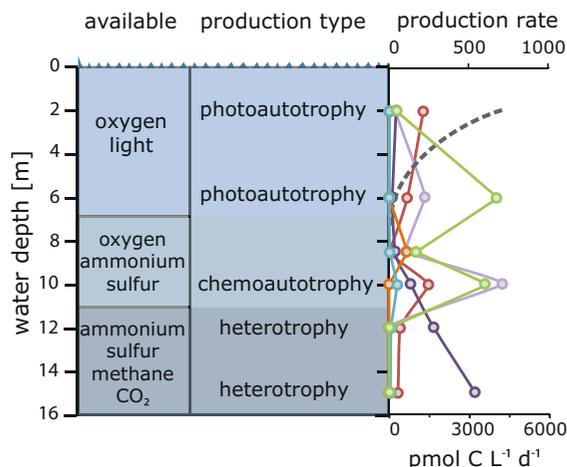
Fig. 7 Conceptual plot of dominant production types recognized at different depths (*middle*). On the *left*, available sources for production are shown; on the *right*, production rates in pmol C L^{-1} d^{-1} of producers versus depth are shown. The *dashed grey line* represents best guess cyanobacterial production (not quantified directly, but based on missing sink), the *green line* represents photoautotrophy, the *blue line* mixotrophy, the *orange line* chemoautotrophy and the *red line* heterotrophy. Autotrophic production of C16:1ω7c is represented by the *light purple line* while heterotrophic production of C16:1ω7c is shown in *dark purple*. Both shades of *purple* are plotted on the secondary axis at the *bottom*. (Color figure online)

with different PLFAs produced at different depths (Fig. 5). Using PLFAs, we were able to show that high concentrations, or large biomass, does not necessarily indicate high production rates (Figs. 3, 5), which would otherwise have required several sampling campaigns.

These findings have implications for monitoring carbon flows in lakes and linking activity and identity of organisms. Total particulate primary production (POC production) showed clear depth-dependence linked to light penetration, but the communities involved differed. Cyanobacteria dominated the upper layer, eukaryotic phytoplankton the subsurface water and a distinct low-light community was able to fix inorganic carbon at 10 m depth. There was also depth zonation in extracellular carbon release and heterotrophic bacterial growth on recently fixed carbon. Accordingly, lake monitoring programs based on one single depth provide an incomplete picture of the diversity and dynamics of photoautotrophs in this type of lakes. In lakes such as Rotsee, where light penetration and the oxycline occur at similar depths, one would expect and we have found that a diversity of

communities is involved in carbon cycling (low-light phototrophs, chemo-autotrophs, mixotrophs, methanotrophs and heterotrophs) (Fig. 7).

References

Battin TJ, Kaplan LA, Findlay S, Hopkinson CS, Marti E, Packman AI, Newbold JD, Sabater F (2008) Biophysical controls on organic carbon fluxes in fluvial networks. Nat Geosci 1:95–100

Battin TJ, Luyssaert S, Kaplan LA, Aufdenkampe AK, Richter A, Tranvik LJ (2009) The boundless carbon cycle. Nat Geosci 2:598–600

Bauersachs T, Compaoré J, Hopmans EC, Stal LJ, Schouten S, Sinninghe Damsté JS (2009) Distribution of heterocyst glycolipids in cyanobacteria. Phytochemistry 70:2034–2039

Bloesch J, Stadelmann P, Buhrer H (1977) Primary production, mineralization, and sedimentation in the euphotic zone of two swiss lakes. Limnol Oceanogr 22:511–526

Bodelier PLE, Bär Gillisen MJ, Hordijk K, Sinninghe Damsté JS, Rijpstra WIC, Geenevasen JAJ, Dunfield P (2009) A reanalysis of phospholipid fatty acids as ecological biomarkers for methanotrophic bacteria. ISME J 3:606–617

Boschker HTS, Nold SC, Wellsbury P, Bos D, de Graaf W, Pel R, Parkes RJ, Cappenberg TE (1998) Direct linking of microbial populations to specific biogeochemical processes by ^{13}C-labelling of biomarkers. Nature 392: 801–805

Boschker HTS, Moerdijk-Poortvliet TCW, van Breugel P, Houtekamer M, Middelburg JJ (2008) A versatile method for stable carbon isotope analysis of carbohydrates by high-performance liquid chromatography/isotope ratio mass spectrometry. Rapid Commun Mass Spectom 22: 3902–3908

Bossard PP, Stettler R, Bachofen R (2000) Seasonal and spatial community dynamics in the meromictic Lake Cadagno. Arch Microbiol 174:168–174

Bowman JP, Skerratt JH, Nichols PD, Sly LI (1991) Phospho-
lipid fatty acid and lipopolysaccharide fatty acid signature
lipids in methane-utilizing bacteria. FEMS Microbiol Ecol
85:15–22

Bowman JP, Sly LI, Nichols PD, Hayward AC (1993) Revised
taxonomy of the methanotrophs—description of *Methy-
lobacter* gen.nov., emendation of *Methylococcus*, valida-
tion of *Methylosinus* and *Methylocystis* species, and a
proposal that the family *Methylococcaceae* includes only
the group-I methanotrophs. Int J Syst Bacteriol 43:735–753

Brand A, Bruderer H, Oswald K, Guggenheim C, Schubert CJ,
Wehrli B (2016) Oxygenic primary production below the
oxycline and its importance for redox dynamics. Aquat Sci.
doi:10.1007/s00027-016-0465-4

Brett MT, Kainz MJ, Taipale SJ, Seshan H (2009) Phyto-
plankton, not allochthonous carbon, sustains herbivorous
zooplankton production. PNAS 106:21197–21201

Cole JJ, Pace ML, Carpenter SR, Kitchell JF (2000) Persistence
of net heterotrophy in lakes during nutrient addition and
food web manipulations. Limnol Oceanogr 45:1718–1730

Cole JJ, Carpenter SR, Pace ML, van de Bogert C, Kitchell JF,
Hodgson JR (2006) Differential support of lake food webs
by three types of terrestrial organic carbon. Ecol Lett
9:558–568

Cole JJ, Prairie YT, Caraco NF, McDowell WH, Tranvik LJ,
Striegl RG, Duarte CM, Kortelainen P, Downing JA,
Middelburg JJ, Melack JM (2007) Plumbing the global
carbon cycle: integrating Inland waters into the terrestrial
carbon budget. Ecosystems 10:171–184

Cole JJ, Carpenter SR, Kitchell JF, Pace ML, Solomon CT,
Weidel BC (2011) Strong evidence for terrestrial support
of zooplankton in small lakes based on stable isotopes of
carbon, nitrogen, and hydrogen. PNAS 108:1975–1980

Coplen TB (2011) Guidelines and recommended terms for
expression of stable-isotope-ratio and gas-ratio measure-
ment results. Rapid Commun Mass Spectrom 25:2538–2560

de Bie MJM, Starink M, Boschker HTS, Peene JJ, Laanbroek HJ
(2002) Nitrification in the Schelde estuary: methodological
aspects and factors influencing its activity. FEMS Micro-
biol Ecol 42:99–107

De Kluijver A, Soetaert K, Czerny J, Schulz KG, Boxhammer T,
Riesebell U, Middelburg JJ (2013) A ^{13}C labelling study on
carbon fluxes in Arctic plankton communities under ele-
vated CO_2 levels. Biogeosciences 10:1425–1440

Del Giorgio PA, Cole JJ (1998) Bacterial growth efficiency in
natural aquatic systems. Annu Rev Ecol Syst 29:503–541

Del Giorgio PA, Peters RH (1994) Patterns in planktonic P: r
ratios in lakes: influence of lake trophy and dissolved
organic carbon. Limnol Oceanogr 39:772–787

Del Giorgio PA, Cole JJ, Cimberlis A (1997) Respiration rates
in bacteria exceed phytoplankton production in unpro-
ductive systems. Nature. doi:10.1038/385148a0

Dickson L, Bull ID, Gates PJ, Evershed RP (2009) A simple
modification of a silicic acid lipid fractionation protocol to
eliminate free fatty acids from glycolipid and phospholipid
fractions. J Microbiol Methods 78:249–254

Dijkman NA, Kromkamp JC (2006) Phospholipid-derived fatty
acids as chemotaxonomic markers for phytoplankton:
application for inferring phytoplankton composition. Mar
Ecol Prog Ser 324:113–125

Dijkman NA, Boschker HTS, Middelburg JJ, Kromkamp JC
(2009) Group-specific primary production based on stable-
isotope labeling of phospholipid-derived fatty acids. Lim-
nol Oceanogr Methods 7:612–625

Fogg GE (1983) The ecological significance of extracellular
products of phytoplankton photosynthesis. Bot Mar
26:3–14

Galand PE, Saarnio S, Fritze H, Yrjälä K (2002) Depth related
diversity of methanogen Archaea in Finnish oligotrophic
fen. FEMS Microbiol Ecol 42:441–449

Guckert JB, Ringelberg DB, White DC, Hanson RS, Bratina BJ
(1991) Membrane fatty acids as phenotypic markers in the
polyphasic taxonomy of methylotrophs within the Pro-
teobacteria. J Gen Microbiol 137:2631–2641

Guezennec J, Fialamedioni A (1996) Bacterial abundance and
diversity in the Barbados trench determined by phospho-
lipid analysis. FEMS Microbiol Ecol 19:83–93

Gugger M, Lyra C, Suominen I, Tsitko I, Humbert JF, Salkinoja-
Salonen MS, Sivonen K (2002) Cellular fatty acids as
chemotaxonomic markers of the genera *Anabaena*, *Apha-
nizomenon*, *Microcystis*, *Nostoc* and *Planktothrix*
(cyanobacteria). Int J Syst Evol Microbiol 52:1007–1015

Hama T, Miyazaki T, Ogawa Y, Iwakuma T, Takahashi M,
Otsuki A, Ichimura S (1983) Measurement of photosyn-
thetic production of a marine phytoplankton population
using a stable ^{13}C isotope. Mar Biol 73:31–36

Humayoun SB, Bano N, Hollibaugh JT (2003) Depth distribution
of microbial diversity in Mono Lake, a meromictic soda lake
in California. Appl Environ Microbiol 69:1030–1042

Jones HLJ, Leadbeater BSC, Green JC (1994) The haptophyte
algae. Systematics Association and Clarendon Press,
Oxford

Kaneda T (1991) Iso-fatty and anteiso-fatty acids in bacteria—
biosynthesis, function and taxonomic significance.
Microbiol Rev 55:288–302

Koizumi Y, Kojima H, Oguri K, Kitazato H, Fukui M (2004)
Vertical and temporal shifts in microbial communities in
the water column and sediment of saline meromictic Lake
Kaiike (Japan), as determined by a 16S rDNA-based
analysis, and related to physicochemical gradients. Envi-
ron Microbiol 6(6):622–637

Lewin JC (1953) Heterotrophy in diatoms. J Gen Microbiol
9:305–313

Lipski A, Spieck E, Makolla A, Altendorf K (2001) Fatty acid
profiles of nitrite-oxidizing bacteria reflect their phyloge-
netic heterogeneity. Syst Appl Microbiol 24:377–384

Middelburg JJ (2014) Stable isotopes dissect aquatic food webs
from the top to the bottom. Biogeosciences 11:2357–2371

Middelburg JJ, Barranguet C, Boschker HTS, Herman PMJ,
Moens T, Heip CHR (2000) The fate of intertidal micro-
phytobenthos carbon: an in situ ^{13}C-labeling study. Limnol
Oceanogr 45:1224–1234

Morana C, Roland FAE, Crowe SA, Llirós M, Borgers AV,
Darchambeau F, Bouillon S (2016) Chemoautotrophy and
anoxygenic photosynthesis within the water column of a
large meromictic tropical lake (Lake Kivu, East Africa).
Limnol Oceanogr 61:1424–1437

Naeher S, Peterse F, Smittenberg RH, Niemann H, Zigah PK,
Schubert CJ (2014) Sources of glycerol dialkyl glycerol
tetraethers (GDGTs) in catchment soils, water column and

sediments of Lake Rotsee (Switzerland)—implications for the application of GDGT-based proxies for lakes. Org Geochem 66:164–173

Necchi O Jr, Zucchi MR (2001) Photosynthetic performance of freshwater Rhodophyta in response to temperature, irradiance, pH and diurnal rhythm. Phycol Res 49:305–318

Nichols PD, Smith GA, Antworth CP, Hanson RS, White DC (1985) Phospholipid and lipoploysaccharide normal and hydroxy fatty-acids as potential signatures for methane-oxidizing bacteria. FEMS Microbiol Ecol 31:327–335

Oswald K, Milucka J, Brand A, Littmann S, Wehrli B, Kuypers MMM, Schubert CJ (2015) Light-dependent aerobic methane oxidation reduces methane emissions from seasonally stratified lakes. PLoS ONE 10(7):e0132574

Øvreås L, Forney L, Daae FL, Torsvik V (1997) Distribution of bacterioplankton in meromictic Lake Saelenvannet, as determined by denaturing gradient gel electrophoresis of PCR-amplified gene fragments coding for 16S rRNA. Appl Environ Microbiol 63:3367–3373

Pace ML, Prairie YT (2005) Respiration in lakes. In: del Giorgio PA, Williams PJl (eds) Respiration in Aquatic Ecosystems. Oxford University Press Inc, New York, pp 103–121

Pace ML, Cole JJ, Carpenter SR, Kitchell JF, Hodgson JR, van de Bogert C, Bade DL, Kritzberg ES, Bastviken D (2004) Whole-lake carbon-13 additions reveal terrestrial support of aquatic food webs. Nature 427:240–243

Pace ML, Carpenter SR, Cole JJ, Coloso JJ, Kitchell JF, Hodgson JR, Middelburg JJ, Preston ND, Solomon CT, Weidel BC (2007) Does terrestrial organic carbon subsidize the planktonic food web in a clear-water lake? Limnol Oceanogr 52:2177–2189

Prairie YT, Bird DF, Cole JJ (2002) The summer metabolic balance in the epilimnion of southeastern Quebec lakes. Limnol Oceanogr 47:316–321

Raymond PA, Hartmann J, Lauerwald R, Sobek S, McDonald C, Hoover M, Butman D, Striegl RG, Mayorga E, Humborg C, Kortelainen P, Dürr H, Meybeck M, Ciais P, Guth P (2013) Global carbon dioxide emissions from inland waters. Nature 503:355–387

Richey JE, Melack JM, Aufdenkampe AK, Ballester VM, Hess LL (2002) Outgassing from Amazonian rivers and wetlands as a large tropical source of atmospheric CO_2. Nature 416:617–621

Roberts EC, Laybourn-Parry J (1999) Mixotrophic cryptophytes and their predators in the Dry Valley lakes of Antarctica. Freshw Biol 41:737–746

Sanders RW, Porter KG (1988) Phagotrophic phytoflagellates. Adv Microb Ecol 10:167–192

Schubert CJ, Lucas FS, Durisch-Kaiser E, Stierli R, Diem T, Scheidegger O, Vazquez F, Müller B (2010) Oxidation and emission of methane in a monomictic lake (Rotsee, Switzerland). Aquat Sci 72:455–466

Scott JH, O'Brien DM, Emerson D, Sun H, McDonald GD, Salgado A, Fogel ML (2006) An examination of the carbon isotope effects associated with amino acid biosynthesis. Astrobiology 6:867–880

Shishlyannikov SM, Klimenkov IV, Bedoshvili YD, Mikhailov IS, Gorshkov AG (2014) Effect of mixotrophic growth on the ultrastructure and fatty acid composition of the diatom Synedra acus from Lake Baikal. J Biol Res Thessalon 21:15

Smith WOJ, Barber RT, Huntsman SA (1977) Primary production off the coast of northwest Africa: excretion of dissolved organic matter and its heterotrophic uptake. Deep-Sea Res 24:35–47

Taipale SJ, Strandberg U, Peltomaa E, Galloway AWE, Ojala A, Brett MT (2013) Fatty acid composition as biomarkers of freshwater microalgae: analysis of 37 strains of microalgae in 22 genera and in seven classes. Aquat Microb Ecol 71:165–178

Tan CK, Johns MR (1996) Screening of diatoms for heterotrophic eicosapentaenoic acid production. J Appl Phycol 8:59–64

Tranvik LJ, Downing JA, Cotner JB, Loiselle SA, Striegl RG, Ballatore TJ, Dillon P, Finlay K, Fortino K, Knoll LB, Kortelainen PL, Kutser T, Larsen S, Laurion I, Leech DM, Leigh McCallister SL, McKnight DM, Melack JM, Overholt E, Porter JA, Prairie Y, Renwick WH, Roland F, Sherman BS, Schindler DW, Sobek S, Tremblay A, Vanni MJ, Verschoor AM, von Wachenfeldt E, Weyhenmeyer GA (2009) Lakes and reservoirs as regulators of carbon cycling and climate. Limnol Oceanogr 65:2298–2314

Travers M, Shin YJ, Jennings S, Cury P (2007) Towards end-to-end models for investigating the effects of climate and fishing in marine ecosystems. Prog Oceanogr 75:751–770

Van den Meersche K, Middelburg JJ, Soetaert K, van Rijswijk P, Boschker HTS, Heip CHR (2004) Carbon-nitrogen coupling and algal-bacterial interactions during an experimental bloom: modeling a ^{13}C tracer experiment. Limnol Oceanogr 49:862–878

van Gaever S, Moodley L, Pascotti F, Houtekamer M, Middelburg JJ, Danovaro R, Vanreusel A (2009) Trophic specialisation of metazoan meiofauna at the Håkon Mosby Mud Volcano: fatty acid biomarker isotope evidence. Mar Biol 156:1289–1296

White DC, David WM, Nickels JS, King JD, Bobbie RJ (1979) Determination of the sedimentary microbial biomass by extractible lipid phosphate. Oecologia 40:51–62

Wright RT, Shah NM (1975) The trophic role of glycolic acid in coastal seawater. I. Heterotrophic metabolism in seawater and bacterial cultures. Mar Biol 33:175–183

Zelles L (1999) Fatty acid patterns of phospholipids and lipopolysaccharides in the characterisation of microbial communities in soil: a review. Biol Fertil Soils 29:111–129

Zepp Falz K, Holliger C, Grosskopf R, Liesack W, Nozhevnikova AN, Müller B, Wehrli B, Hahn D (1999) Vertical distribution of methanogens in the anoxic sediment of Rotsee (Switzerland). Appl Environ Microbiol 65:2402–2408

Zhang CL, Huang Z, Cantu J, Pancost RD, Brigmon RL, Lyons TW, Sassen R (2005) Lipid biomarkers and carbon isotope signatures of a microbial (Beggiatoa) mat associated with gas hydrates in the gulf of Mexico. Appl Environ Microbiol 71:2106–2112